ISSN 1027-5495. Functional Materials, 30, No.3 (2023), p. 356-362.
doi:https://doi.org/10.15407/fm30.03.356

A new Cu(II) complex constructed from 4-[(8-hydroxy-5-quinolinyl) azo]-benzoic acid: synthesis, crystal structure and antibacterial property

***Yanan Luo*[1], *Hongxu Bai*[2], *Hongri Fan*[3], *Liying Yu*[2], *Heyun Zhu*[1], *Jiamu Song*[1], *Jiao Guan*[1]**

[1]College of Pharmacy, Jilin Medical University, 5 Jilin Str., 132013 Jilin, P. R. China
[2]College of Chemical and Pharmaceutical Engineering, Jilin Institute of Chemical Technology, 45 Chengde Str., 132022 Jilin, P. R. China
[3]Guangxi Vocational & Technical Institute of Industry, 37 Xiuling Str., 530001 Guangxi, P. R. China

Received June 25, 2023

By using 4-[(8-hydroxy-5-quinolinyl) azo]-benzoic acid (H_2L) ligand, a new inorganic-organic hybrids, formulated as $[Cu(HL^-)_2]\cdot 2DMA$ (**1**) (DMA = N,N-Dimethylacetamide), has been synthesized successfully under conventional solvothermal conditions. Complex **1** exhibits a zero-dimensional (0D) structure, which is linked into a one-dimensional (1D) supramolecular network by π–π stacking interaction. In addition, the antibacterial property of complex **1** was tested. The antibacterial property of complex **1** in relation to Gram-positive bacteria is slightly better than in relation to Gram-negative bacteria in complex 1.

Keywords: solvothermal conditions, supramolecular network, antibacterial property, π–π stacking interaction.

Новий комплекс Cu(II), побудований з 4-[(8-гідрокси-5-хінолініл)азо]-бензойної кислоти: синтез, кристалічна структура та антибактеріальні властивості. *Yanan Luo, Hongxu Bai, Hongri Fan, Liying Yu, Heyun Zhu, Jiamu Song, Jiao Guan*

З використанням ліганду 4-[(8-гідрокси-5-хінолініл)азо]-бензойної кислоти (H_2L) був успішно синтезований новий неорганічно-органічний гібрид, сформульований як $[Cu(HL^-)_2]\cdot 2DMA$ (1) (DMA = N,N-диметилацетамід) в звичайних сольвотермічних умовах. Комплекс **1** має нульвимірну (0D) структуру, яка пов'язана з одновимірною (1D) супрамолекулярною сіткою через π–π стекінг-взаємодію. Крім того, було перевірено антибактеріальну властивість комплексу **1**. Антибактеріальні властивості комплексу **1** дещо кращі проти грампозитивних бактерій, ніж проти грамнегативних бактерій.

1. Introduction

In recent years, with the continuous research on metal organic framework materials, more and more functional properties have been discovered [1–3]. Studies have appeared on the use of organometallic scaffold materials in solid antibacterial agents [4]. Among them, the mechanism that may produce antibacterial effects has also attracted wide attention [5]. After extensive research, it has been found that the main mechanisms of action of metal organic framework materials in antibacterial aspects can be summarized into the following

three situations [6–8]. The first is the structural degradation of metal organic frameworks. The second is the slow release of metal center ions in metal organic framework materials. The third is the reaction between metal organic framework materials and surface-active antibacterial metals. These are all the main reasons that may cause antibacterial activity. Among the reported metal organic framework materials, silver, zinc, copper, cobalt and nickel ions are common metal central ions with antibacterial functions [9, 10]. These antibacterial crystal materials have been tested for antibacterial activity in both Gram-negative Escherichia coli (E. coli) and Gram-positive Staphylococcus aureus (S. aureus) [11]. In 2017, Jimmy Restrepo et al. synthesized a three-dimensional porous zinc-based metal organic framework crystal material using hydrazine benzoic acid as an organic ligand. The crystalline material has a certain antibacterial effect on gram-positive S. aureus, which inhibits bacterial growth and metabolic activity. The maximum effective inhibitory concentration is about 20 mg/L. The results showed that the antibacterial mechanism was associated with the release of the organic ligand hydrazine benzoic acid in the crystalline material, which destroyed the cells of S. aureus and resulted in an antibacterial effect [12]. Among them, the release of zinc ions also plays a certain antibacterial role, but the effect is weaker than that of organic ligands. In order to further understanding the antimicrobial mechanism of metal organic framework crystal materials, many studies are still ongoing [13].

In this paper, the complex $[Cu(HL^-)_2]\cdot 2DMA$ (**1**) was successfully synthesized with 4-[(8-hydroxy-5-quinoline) azo]-benzoic acid. Complex **1** was determined by single-crystal X-ray diffraction, elemental analysis, thermogravimetric analysis and powder X-ray diffraction. Finally, the antibacterial property of complex **1** was investigated by using the bacteriostatic method and the growth curve method.

2. Experimental

Synthesis of ligand H_2L. H_2L, 4-[(8-hydroxy-5-quinolinyl) azo]-benzoic acid, was prepared according to the literature method [14].

Synthesis of $[Cu(HL^-)_2]\cdot 2DMA$ (**1**). Complex **1** was synthesized by $Cu(NO_3)_2$ and H_2L under conventional solvothermal conditions. A mixture of H_2L (5 mg, 0.017 mmol), $Cu(NO_3)_2$ (30 mg, 0.16 mmol), DMA (12 mL) was dissolved at room temperature for 1 h until a clear red solution formed. The pH value of the above mixture was adjusted to pH = 6.5 with 2 mol/L HCl. The mixture was kept stirring for 1 h at room temperature, finally put into a Teflon-lined autoclave and kept under autogenous pressure at 130°C for 72 h. After slow cooling to room temperature, red rod crystals were filtered and washed with MDA and dried. For $C_{40}H_{38}CuN_8O_8$ (Mr = 822.32): C 58.42; H 4.66; N 13.63; found: C 58.38; H 4.74; N 13.58.

Structure determination. Complex **1** was stable under ambient conditions and single crystals were glued on thin glass fibers. Diffraction intensities were measured with a Bruker Apex II CCD area-detector diffractometer (Mo Kα, 0.071073 nm). An empirical absorption correction was applied to the data using the SADABS program. The structure was solved by the direct method (SHELXS-97) and refined by full matrix least squares [15]. The distribution of all non-hydrogen atoms was refined as anisotropic. All hydrogen atoms were located geometrically by the program OLEX-2 [16]. The final formula was derived from crystallographic data combined with elemental and thermogravimetric analyses data. CCDC-2268162 contains the supplementary crystallographic data for this paper.

Testing of antibacterial property. The following solution was prepared for antibacterial experiments. The organic ligand (H_2L) solution with the concentration of 5 mg/mL was prepared by ultrasonic stirring of 50 mg organic ligand in 10 mL distilled water. About 50 mg of complex **1** was stirred in 5 mL of distilled water by ultrasonic agitation to prepare a complex **1** solution with a concentration of 10 mg/mL (solution 1). 2.5 mL of solution 1 was taken into 2.5 mL distilled water and ultrasonically stirred into a complex solution of 5 mg/mL (solution 2). Then 1.5 mL of solution 2 was mixed into 1.5 mL distilled water and ultrasonically stirred into a complex solution of 2.5 mg/mL (solution 3). For ultrasound treatment, filter paper sheets with a diameter of about 6 mm were placed into sterile distilled water, H_2L solution, solution 1, solution 2 and solution 3 respectively. After soaking for 1 h, they were taken out and placed in a clean petri dish. Then they were placed on the aseptic operating table and irradiated by ultraviolet lamp for sterilization. The disc diffusion

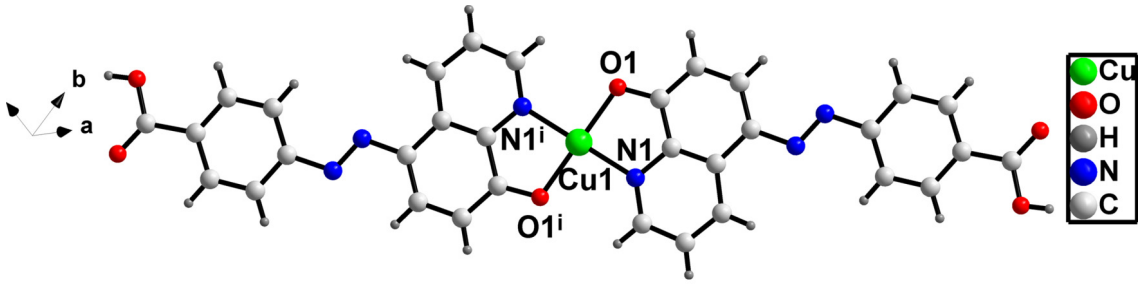

Fig. 1. Coordination environments of Cu1 in complex **1** (symmetry code: i, $-x$, $-y$, $1-z$).

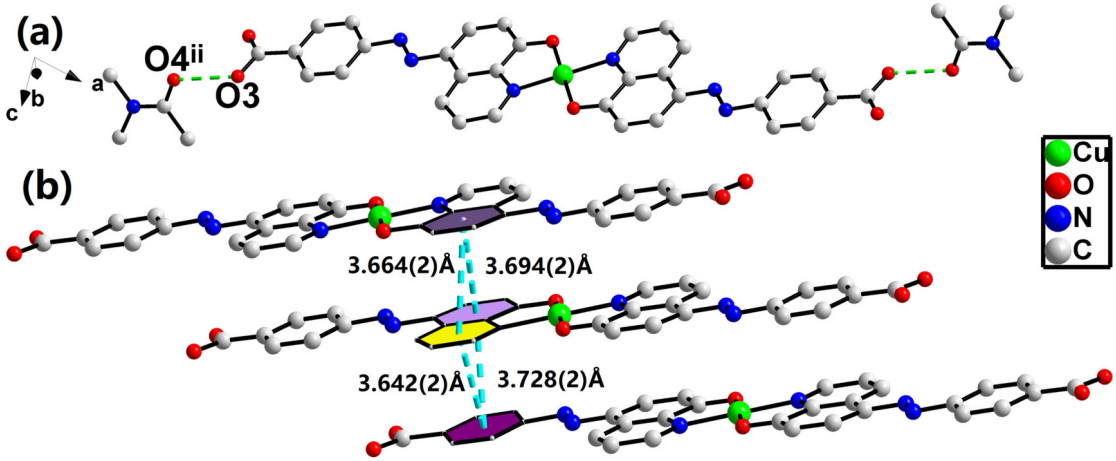

Fig. 2. (a) Complex **1** is linked with an adjacent DMA molecule via hydrogen bonds interactions; (b) 1D chain structure via π–π interactions of complex **1** (symmetry code: ii, 3jx, $-y$, $-z$. All hydrogen atoms are omitted for clarity.

method was used to determine the inhibition zones in the growth of bacterial species. Escherichia coli (ATCC25922) and Staphylococcus aureus (ATCC6538) were selected and inoculated into sterile nutrient agar. After the nutrient agar medium was cooled and shaped, filter papers of the blank water sample, H_2L ligand, solution 1, solution 2 and solution 3 were placed in a fixed position. Seeding was carried out in an incubator with a constant temperature of 37°C for 2–3 days and observed every 6 h.

Gram growth curve experiment.

Complex **1** of different weights was dissolved in the sterilized liquid medium, sealed and stirred by ultrasound. Medium solutions containing complex **1** at concentrations of 0, 6.5, 12.5, 25, 50, 100, 200 and 400 μg/mL were placed in a sterile platform for UV irradiation for sterilization. A certain amount of Staphylococcus aureus culture was inoculated into the liquid medium with the same volume and different concentrations of complex **1**, and placed in an incubator of 37°C. After 0, 3, 6, 9, 12, 16, 18, 21 and 24 h, the absorbance of the above solution (including the same volume of Staphylococcus aureus and different concentrations of complex **1**) was measured by an UV-Vis spectrophotometer at fixed wavelength of 600 nm (according to the literature) [17].

3. Results and discussion

$[Cu(HL^-)_2]\cdot 2DMA$ (**1**) was synthesized by the traditional solvothermal method with $Cu(NO_3)_2$ and H_2L. Single-crystal X-ray diffraction analysis reveals that complex **1** crystallizes in the triclinic crystal system, space group P-1, which exhibits a 0D structure (Table 1). In addition, an asymmetric structural unit of complex **1** contains a Cu(II) ion, an L^- ligand and two crystallization DMA molecules (Fig. 1).

Cu(II) ion is four coordinated by two oxygen atoms and two nitrogen atoms. Among them, Cu1 is coordinated by O1, $O1^i$, N1 and $N1^i$ from two different H_2L molecules, respectively, forming a quadrilateral structure. In complex **1**, the L^- ligand adopted chelation coordination mode. In addition, the bond angle range of Cu1 is [84.88(8)°–

Table 1. Complex **1** of crystal data collections and structure refinements

Complex 1			
Formula	$C_{40}H_{38}CuN_8O_8$	Fw	822.32
Crystal system	triclinic	V/nm^3	0.9456(8)
Temperature, K	293(2)	Space group	*P*-1
α, °	85.86(2)	ρ_{calc}, Mg·m^{-3}	1.444
β, °	80.90(2)	μ, mm^{-1}	0.643
γ, °	68.44(2)	Reflections collected	4814
a, nm	0.7388(3)	*Z*	1
b, nm	0.7773(4)	*F*(000)	427
c, nm	1.7936(8)	θ range (°)	1.150–28.668
Final $R^{a,b}$ indices [$I > 2\sigma(I)$]	R_1 = 0.0509	*R* indices (all data)	R_1 = 0.0784
	wR_2 = 0.1275		wR_2 = 0.1445
Independent reflections (R_{int})	3425(0.0279)	GOF	0.996

Table 2. Selected bond lengths (nm) and angles (°) for complex **1**

Complex 1			
Cu1–O1	0.1932(2)	Cu1–O1^i	0.1932(2)
Cu1–N1i^i	0.1967(2)	Cu1–N1	0.1967(2)
O1–Cu1–O1i^i	180.0	O1–Cu1–N1i^i	95.12(8)
O1i–Cu1–N1i^i	84.88(8)	O1i–Cu1–N1^i	95.12(8)
O1–Cu1–N1^i	84.88(8)	N1–Cu1–N1i^i	180.0

symmetry code for complex 1: *i*, $-x$, $-y$, $1-z$

Table 3. Hydrogen bond distances [nm] and angles [°] in complex **1**

D–H	*d*(D–H)	*d*(H***A)	?DHA	*d*(D–A)	A
O1–H1	0.082	0.180	170	0.2710(7)	O4^{ii}

Symmetry code for complex 1: *ii*, $3-x$, $-y$, $-z$.

180.0°]. The distances of Cu–O/N [0.1932(2)–0.1967(2) nm] are comparable with those found in other related Cu(II) complexes (Table 2).

O3 on the carboxylic acid group is connected with O4^{ii} in the adjacent DMA molecule [*d*(O3O4^{ii}) = 0.2608(5) nm, *angle*O3–H3O4^{ii} = 170°] (Table 3, Fig. 2(a)). In addition, there are abundant π–π stacking interactions in the crystal building (Fig. 2(b)). The range of center distance between 8-hydroxyquinoline and benzene rings was calculated by the Platon program as [3.642(2)–3.728(2)Å], and complex **1** was linked to form a 1D supramolecular chain structure (Table 4).

In order to confirm the structural homogeneity of the bulk power materials, a power X-ray diffraction (PXRD) experiment has been carried out. The PXRD experimental and computer-simulated patterns are in good agreement with each other (Fig. 3), indicating phase purity of complex **1**.

In order to determine the thermal stability of complex **1**, the thermogravimetric analyze has been determined. The experimental results show that the weight loss in the range of 172 to 423°C is consistent with the removal of two crystallization DMA molecules (exp. 20.98 %, cal. 21.19 %). The total weight loss of 69.22 % in the range of 442°C to 938°C can be attributed to the release of two HL^- ligands (cal.

Table 4. Selected π–π interactions geometry for complex **1**

Complex 1						
Cg(I) → Cg(J)	Cg–Cg, ()	α, °	β, °	γ, °	CgI_Perp ()	CgJ_Perp ()
Cg3 → Cg4^{iii}	3.664(2)	1.10(2)	21.17	20.28	3.437(2)	−3.417(2)
Cg3 → Cg5^{iv}	3.642(2)	3.36(2)	16.71	14.55	3.525(2)	−3.488(2)
Cg4 → Cg4^{iii}	3.694(2)	0	22.49	22.49	3.413(2)	3.413(2)
Cg4 → Cg5^{iv}	3.728(2)	4.19(2)	20.53	24.46	3.394(2)	−3.492(2)

Cg(I) = Plane number I (= ring number in () above) (Cg3 = N1 → C1 → C2 → C3 → C4 → C5; Cg4 = C4 → C5 → C6 → C7 → C8 → C9; Cg5 = C10 → C11 → C12 → C13 → C14 → C15) (Symmetry codes for complex **1**: iii, 1−*x*, −*y*, 1−*z*; iv, −1+*x*, *y*, *z*)
Cg–Cg = Distance between ring Centroids (Ang.)
α = Dihedral Angle between Planes I and J (Deg)
β = Angle Cg(I) → Cg(J) or Cg(I) → Me vector and normal to plane I (Deg)
γ = Angle Cg(I) → Cg(J) vector and normal to plane J (Deg)
CgI_Perp = Perpendicular distance of Cg(I) on ring J (Ang.)

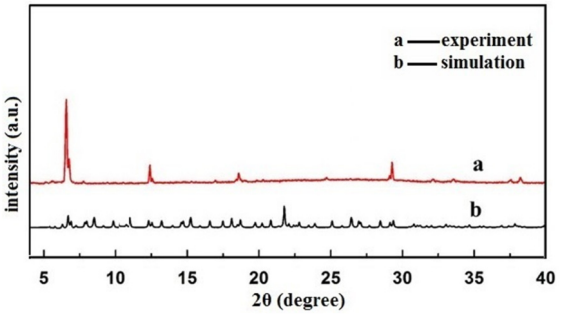

Fig. 3. Experimental (a) and simulative (b) powder X-ray diffraction patterns for complex **1**.

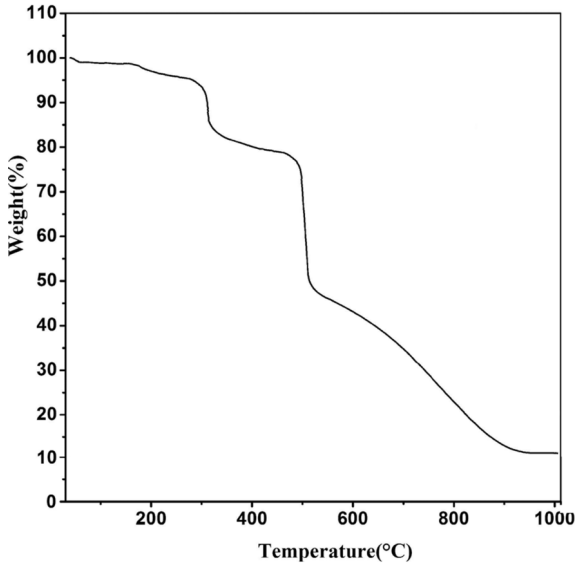

Fig. 4. TGA curve of complex **1**.

69.14 %). According to the weight loss analysis, the final product may be CuO (exp. 9.72 %, cal. 9.67 %) (Fig. 4).

As shown in Fig. 5(a) and (b), the antibacterial activity of complex 1 was studied against gram-negative E. coli and gram-positive S. aureus. The results showed that blank filter paper with H_2L ligand had no antibacterial activity against E. coli and S. aureus in Petri dishes. The low concentration and high concentration of complex **1** had no antibacterial activity, but the medium concentration had slightly antibacterial activity against E. coli. At the same time, a high concentration of complex **1** showed a relatively high antibacterial activity against S. aureus. In addition, in Fig. 5(a) and (b), it can be seen that complex **1** has a stronger inhibitory effect and a better antibacterial performance against S. aureus compared with E. coli. By comparing the antibacterial activities of H_2L ligand and complex **1** of different concentrations, it was indicated that the ligand itself did not have antibacterial activities, while the inhibition zone of the complex **1** with the concentration of 10 mg/mL was larger than other concentrations. The results indicated that complex **1** had a good antibacterial activity, which was mainly due to the slow release of Cu^{2+} from complex **1**.

In order to further study and verify the antibacterial activities, the effect of complex **1** on the growth of S. aureus was tested. The results showed that the growth curve of S. aureus treated with 6.5, 12.5 and 25 μg/mL complex **1** was almost the same as that treated with 0 μg/mL complex **1**, showing typical growth curve (Fig. 6). Therefore, it was shown that complex **1** had no inhibitory

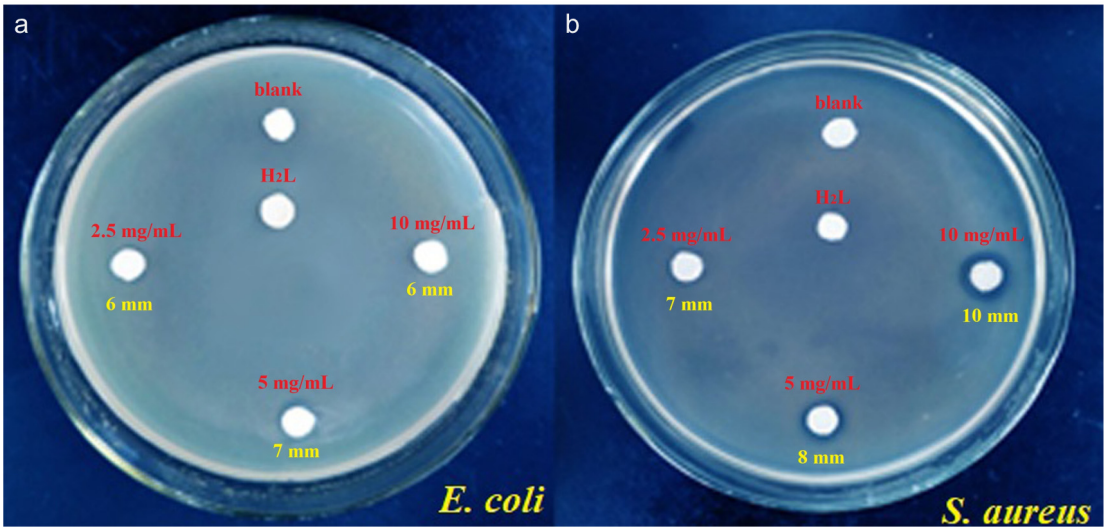

Fig. 5. (a) Optical photograph of complex **1** for negative E. coli; (b) Optical photograph of complex **1** for positive S. aureus.

effect on S. aureus at low mass concentration. OD600 of S. aureus treated with 50, 100, 200 and 400 μg/mL of complex **1** showed no obvious change after about 0–6 h compared with OD600 in the initial stage, indicating that complex **1** had inhibitory effect on the growth of S. aureus. However, with increasing time, the growth trend of S. aureus treated with 50 and 100 μg/mL complex **1** tended to the typical S. aureus growth curve, which indicated that the delay period of S. aureus was prolonged relative to the low concentration. After 24 h treatment, the highest OD600 of S. aureus treated with 50 and 100 μg/mL complex **1** were close to the control group at 0 μg/mL. That is, when S. aureus reached a certain level, complex **1** with a mass concentration 50 and 100 μg/mL could no longer inhibit the growth of S. aureus. Only complex **1** with mass concentrations more than 200 μg/mL could completely inhibit the proliferation and growth of S. aureus in the culture medium within 24 h. Complex **1** is an insoluble solid material, which may be a good solid antibacterial agent.

4. Conclusion

In this paper, a Cu(II)-based coordination polymer $[Cu(HL^{-})_2]\cdot 2DMA$ with the 0D structure was successfully synthesized by solvothermal synthesis using H_2L ligand and Cu(II) ions. The 0D structure is linked into a 1D supramolecular network structure by π–π stacking interaction. Complex **1** showed good antibacterial properties in the inhibitory region of Gram-positive S. aureus. Complex **1**

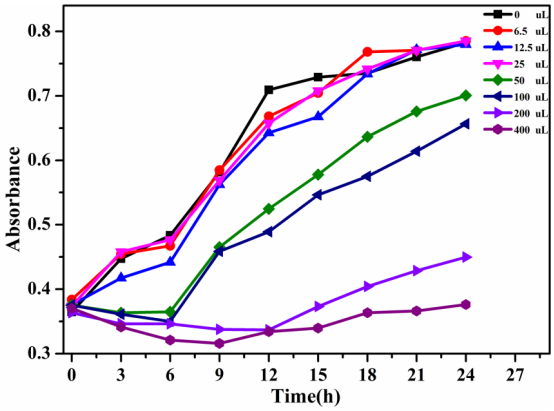

Fig. 6. Growth curves of E. coli for different concentrations of complex **1**.

with mass concentrations above 200 μg/mL could completely inhibit the proliferation and growth of S. aureus in the culture medium within 24 h. This also indicates that the crystalline material of complex **1** has a good potential for applications in the field of biology.

Acknowledgment.

This work was supported by the National Science Foundation of China (grant No. 21902058), Natural Science Foundation of Jilin Province (No. 20180101191JC), the Major Project in Jilin Institute of Chemical Technology (No. 2018021),the Project in Jilin Medical University (No. JYBS2021019LK),Project of Science and Technology Development of Jilin City (No. 20190104161), the Science and Technology Project in Jilin Province Department of Education (No. JJKH20220458KJ), Industrial Technology Research and Development Project of Jilin Provincial Development and

Reform Commission (No. 2023C038-5), Scientific Research of Guangxi Vocational & Technical Institute of Industry (No. Y2020KY004).

References

1. S.Kitagawa, K.Uemura, *Inorg. Chem. Soc. Rev.*, **34**, 109 (2005).
2. Z.Ju, D.Cao, L.Qin et al., *Cryst. Eng. Comm.*, **16**, 3917 (2014).
3. P.Horcajada, T.Chalati, C.Serre et al., *Nat. Mater.*, **9**, 172 (2010).
4. S.Yuhong, H.Hong, *Inorg. Chem. Commun.*, **105**, 158 (2019).
5. C.Miao, T.E.Su, *Inorg. Chem. Commun.*, **112**, 1 (2020).
6. S.M.Wu, X.L.Li, Y.Xu et al., *Ceram. Int.*, **44**, 19390 (2018).
7. X.Hw, Z.Gan, S.Fisenko et al., *Dalton T.*, **9**, 9688 (2017).
8. K.P.Bai, L.J.Zhou, G.P.Yang et al., *J. Solid State Chem.*, **287**, 121336 (2020).
9. K.K.Gangu, S.B.Mukkamala, *Synth. React. Inorg. M.*, **46**, 98 (2015).
10. K.K.Gangu, S.Maddila, S.B.Mukkamala et al., *Inorg. Chim. Acta*, **466**, 61 (2016).
11. J.Osterrieth, F.J.David, *Bio. Technol. J.*, **16**, 1 (2020).
12. L.Li, Y.Chen, L.Yang et al., *Coord. Chem. Rev.*, **411**, 213 (2020).
13. V.R.Maria, F.Balas, D.Arcos, *Angew. Chem. Int. Ed.*, **46**, 7548 (2007).
14. J.S.Park, S.Jeong, S.Dho et al., *Dyes Pigments*, **87**, 4954 (2010).
15. O.V.Dolomanov, L.J.Bourhis, R.J.Gildea et al., *J. Appl. Crystallogr.*, **42**, 339 (2009).
16. G.M.Sheldrick. SHELXTL NT Crystal Structure Analysis Package[CP]. Version 5.10; Bruker AXS, Analytical X-ray System: Madison, WI (1999).
17. X.J.Duan, X.D.Du, B.B.Zhang et al., *J. Med. Biol. Eng.*, **19**, 237 (2015).